Practical SVBRDF Acquisition of 3D Objects with Unstructured Flash Photography

Recent Advances in 3D Computer Vision

Muhammed Alperen Özkan

06.10.2020

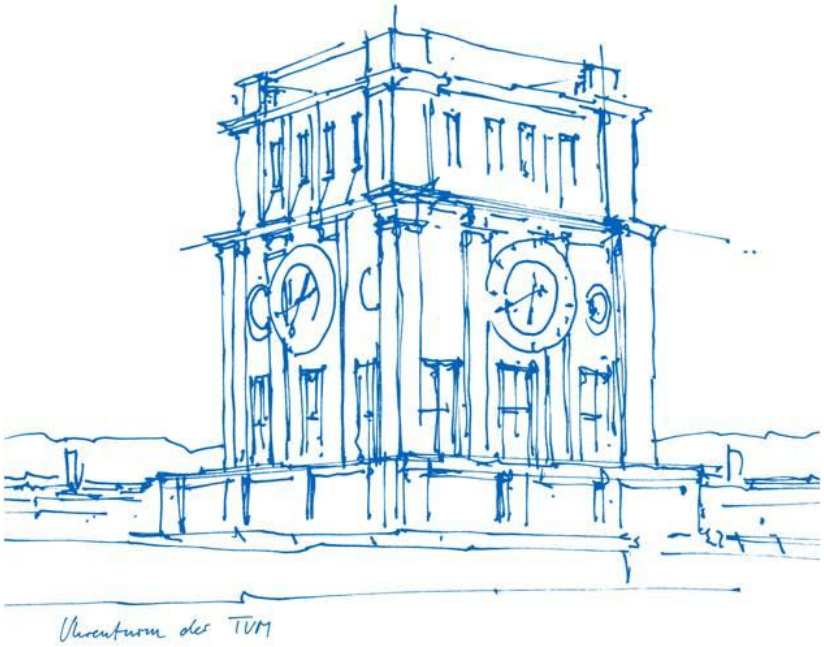

Overview

1. Prior Knowledge
2. Introduction
3. Method in Overall
4. Method in Detail
5. Results and Evaluation
6. Limitations
7. Conclusion

1. Prior Knowledge

Appearance is an interplay of

- surface geometry
- material properties
- illumination characteristics

Figure 1. Red apples and glasses with juice on grey table, by atlascompany, 2020, retrieved from https://image.freepik.com/free-photo/red-apples-glasses-with-juice-grey-table_185193-2293.jpg

In order to obtain realistic digital objects the geometry and reflectance characteristics of the real world objects need to be understood.

Figure 2. GTO Pontiac - Look Development, by Brian Nathaniel, 2018, retrieved from https://www.youtube.com/watch?v=6FFFG61CNrI

There is no technique for geometry and reflectance acquisition that works for all kind of materials.

- Diffuse surfaces

- Specular surfaces

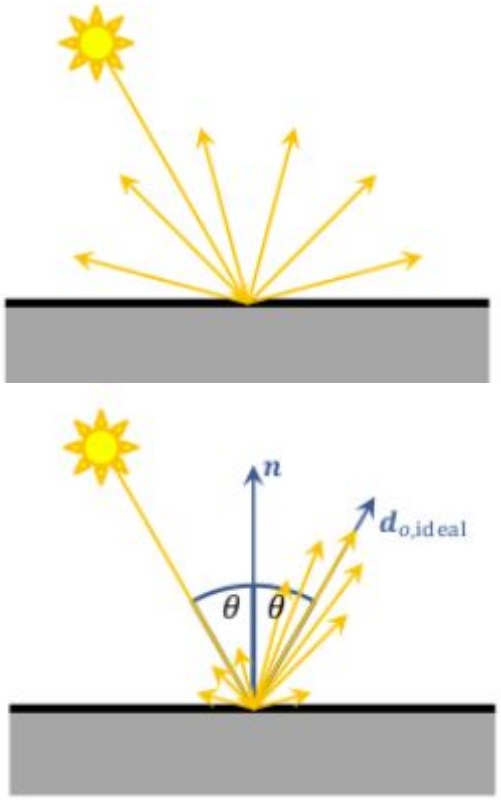

Figure 3. Illustration of different types of surface reflectance behavior for incoming light, Adapted from *Advances in Geometry and Reflectance Acquisition (Course Notes)*, by Weinmann and Klein, 2015, retrieved from https://dl.acm.org/doi/10.1145/2818143.2818165

Radiometry Basics

Light is a form of electromagnetic energy and generally symbolized with rays which can be parameterized with an origin and a direction.

Radiant Flux or Radiant Power is the flow of radiant energy per unit time.

Solid angles are used to describe light being emitted in different directions.

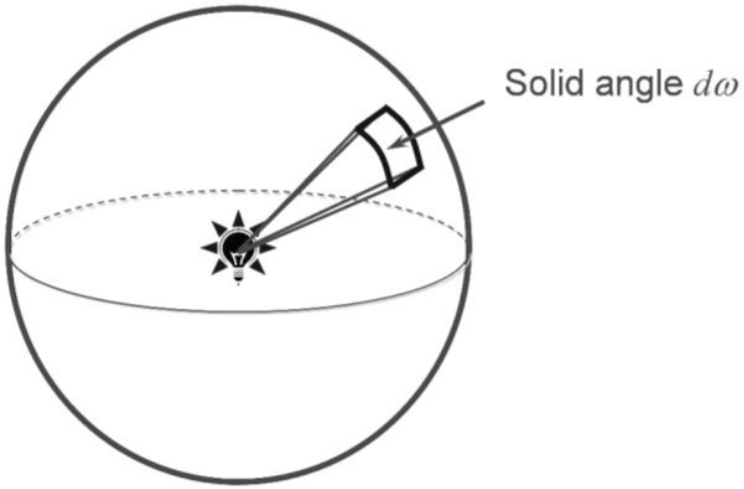

Figure 4. Point light source emitting light in a direction, Adapted from *Principles of Appearance Acquisition and Representation,* by Weyrich et al., 2009, retrieved from https://dl.acm.org/doi/10.1561/0600000022

Irradiance is the amount of light falling onto a surface.

Radiance is the power emitted per unit projected area which is perpendicular to the viewing direction per unit solid angle.

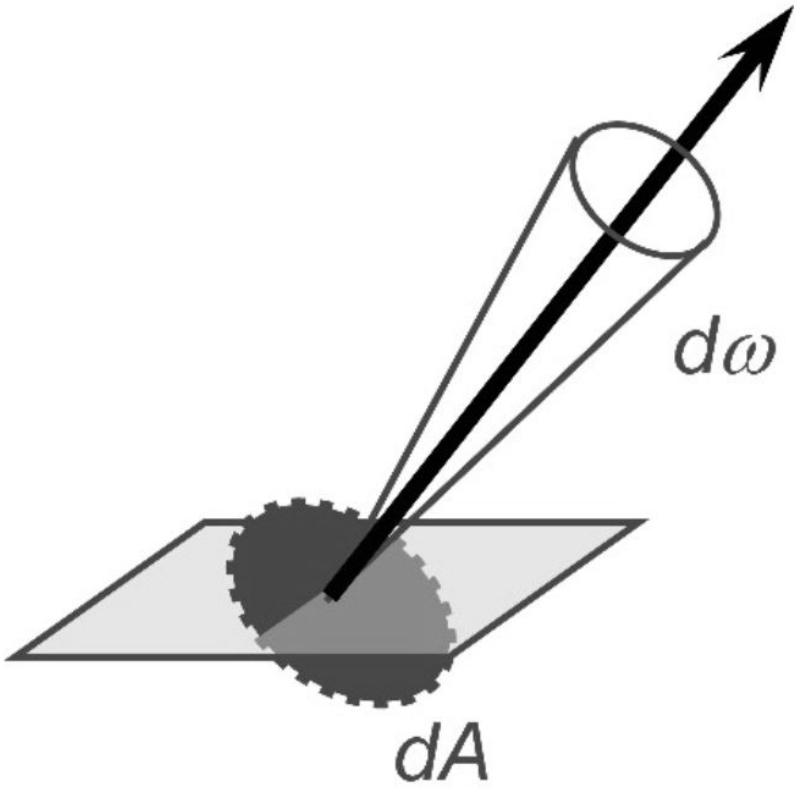

Figure 5. Radiance, Adapted from *Principles of Appearance Acquisition and Representation*, by Weyrich et al., 2009, retrieved from https://dl.acm.org/doi/10.1561/0600000022

Reflectance Functions

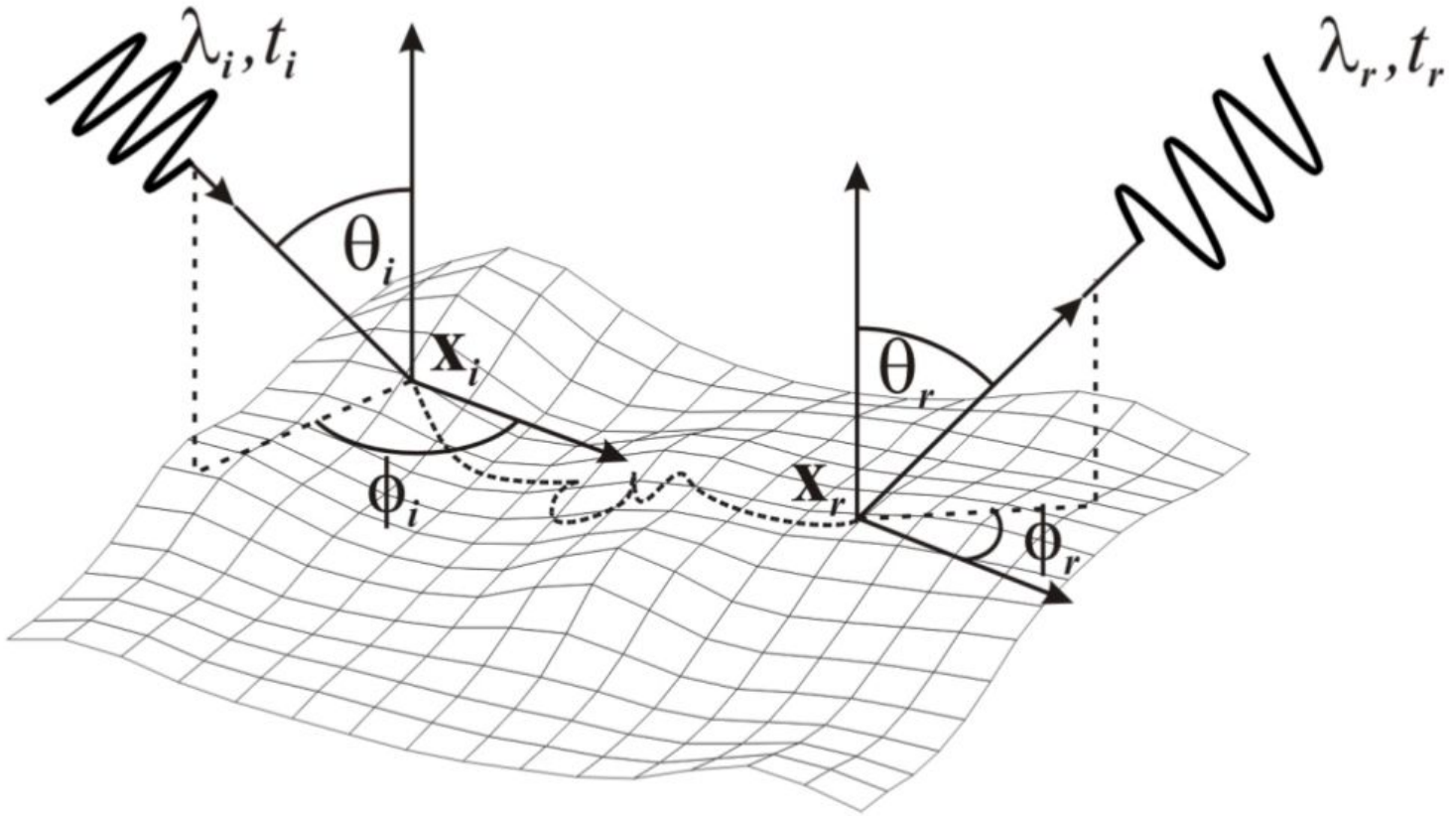

Figure 6. Light exchange at the material surface, Adapted from *Advances in Geometry and Reflectance Acquisition (Course Notes)*, by Weinmann and Klein, 2015, retrieved from https://dl.acm.org/doi/10.1145/2818143.2818165

Bidirectional Reflectance Distribution Function

BRDF is a simple reflectance function that expresses interactions of the light with the surface.

It is the ratio between the reflected radiance of a surface and the irradiance that caused that reflection.

$$f_{\mathrm{r}}(\boldsymbol{\omega}_{\mathrm{i}} \rightarrow \boldsymbol{\omega}_{\mathrm{o}}) = f_{\mathrm{r}}(\theta_{\mathrm{i}}, \varphi_{\mathrm{i}}, \theta_{\mathrm{o}}, \varphi_{\mathrm{o}}) = \frac{dL_{\mathrm{o}}(\boldsymbol{\omega}_{\mathrm{o}})}{dE_{\mathrm{i}}(\boldsymbol{\omega}_{\mathrm{i}})}$$

Spatially Varying Bidirectional Reflectance Distribution Function

Real-world objects generally exhibit more complex behaviors, such as a BRDF that changes from point to point on the surface.

$$SVBRDF(x, y, \theta_{\mathrm{i}}, \varphi_{\mathrm{i}}, \theta_{\mathrm{o}}, \varphi_{\mathrm{o}})$$

2. Introduction

A compact, practical method for 3D geometry and reflectance acquisition by using multiple unstructured flash photographs taken with off-the-shelf cameras as input.

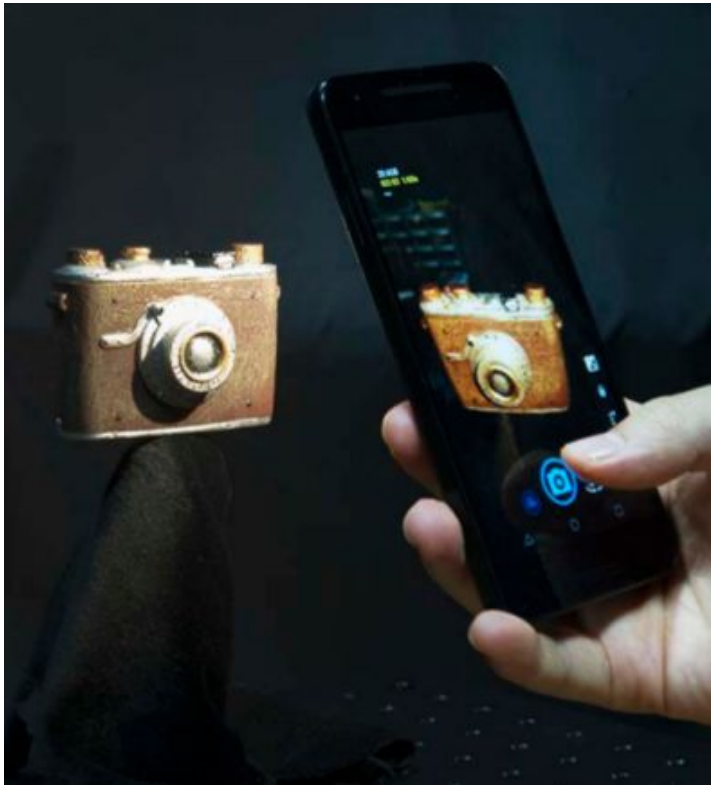

Figure 7. Acquisition setup, Adapted from *Practical SVBRDF Acquisition of 3D Objects with Unstructured Flash Photography,* by Nam et al., 2018, retrieved from https://dl.acm.org/doi/10.1145/3272127.3275017

Prior Work

$$f_r(\omega_i \rightarrow \omega_o) = f_r(\theta_i, \varphi_i, \theta_o, \varphi_o)$$

In order to measure such a BRDF, locally flat surfaces should be illuminated with directed solid angle ω_i and sensors should be placed to subtend an output directed solid angle ω_o.

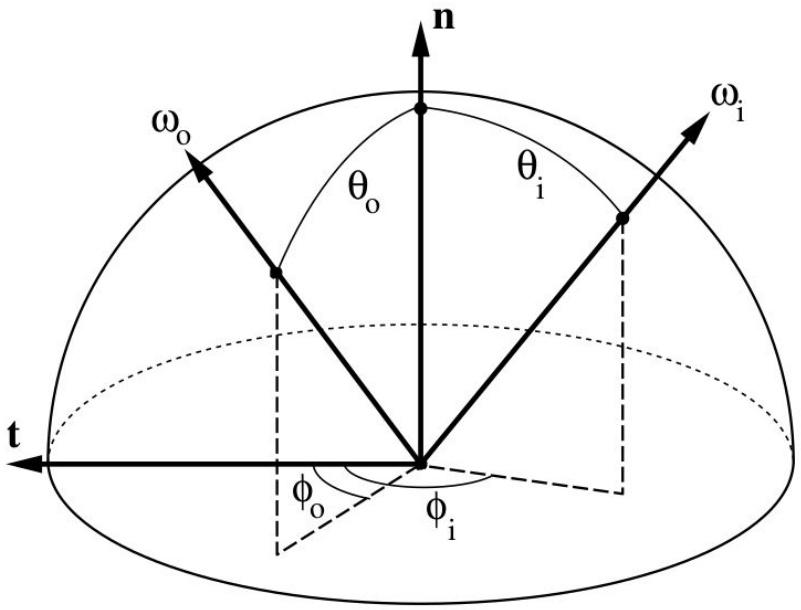

Figure 8. BRDF parameterization, Adapted from *Principles of Appearance Acquisition and Representation, by Weyrich et al., 2009, retrieved from https://dl.acm.org/doi/10.1561/0600000022*

Gonioreflectometers

These specialized devices are not practical and cheap.

Figure 9. Gonioreflectometer, by Robotae, 2017, retrieved from https://www.youtube.com/watch?v=LsfkAbUUXZU

In order to obtain an efficient acquisition,

- arrays of light sources
- digital projectors
- digital cameras

can be used.

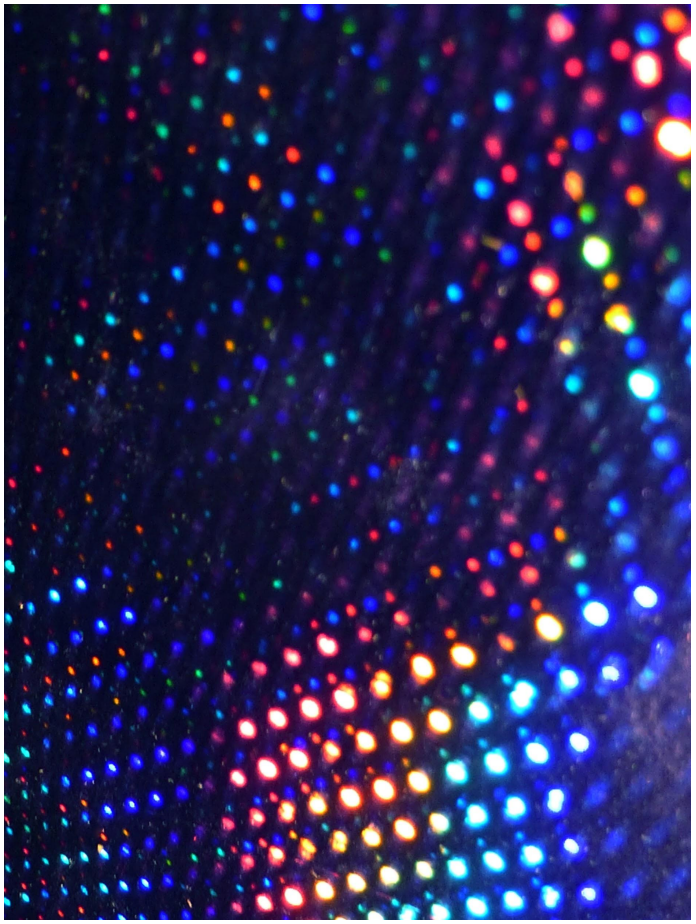

Figure 10. An array of colorful lights creating an unusual design backdrop, retrieved from http://cr103.com/collections/Glow/light_spectrum.jpg

Lightweight Acquisition Setups

There are also lightweight setups but these methods work for near flat 2D objects or make further assumptions about the material characteristics.

- Riviere et al. [2015] and Hui et al. [2017]
- Higo et al. [2009] and Park et al. [2016]

3. Method in Overall

$$O = \sum_{p=1}^{P} \sum_{k=1}^{K} v_{p,k} \left(L(\mathbf{o}_{p,k}; \mathbf{x}_p) - f(\mathbf{i}_{p,k}, \mathbf{o}_{p,k}; \mathbf{x}_p, \mathbf{n}_p) L(-\mathbf{i}_{p,k}; \mathbf{x}_p) (\mathbf{n}_p \cdot \mathbf{i}_{p,k}) \right)^2$$

An inverse-rendering problem is solved with an iterative alternating optimization approach, which updates the four unknown elements

- W →set of blending weights $\{\omega_p, b\}$,
- F_b →set of basis BRDFs $\{f_b\}$,
- N → set of shading normals $\{\tilde{n}_p\}$,
- X → set of 3D points $\{x_p\}$,

until the rendering results satisfy the input images.

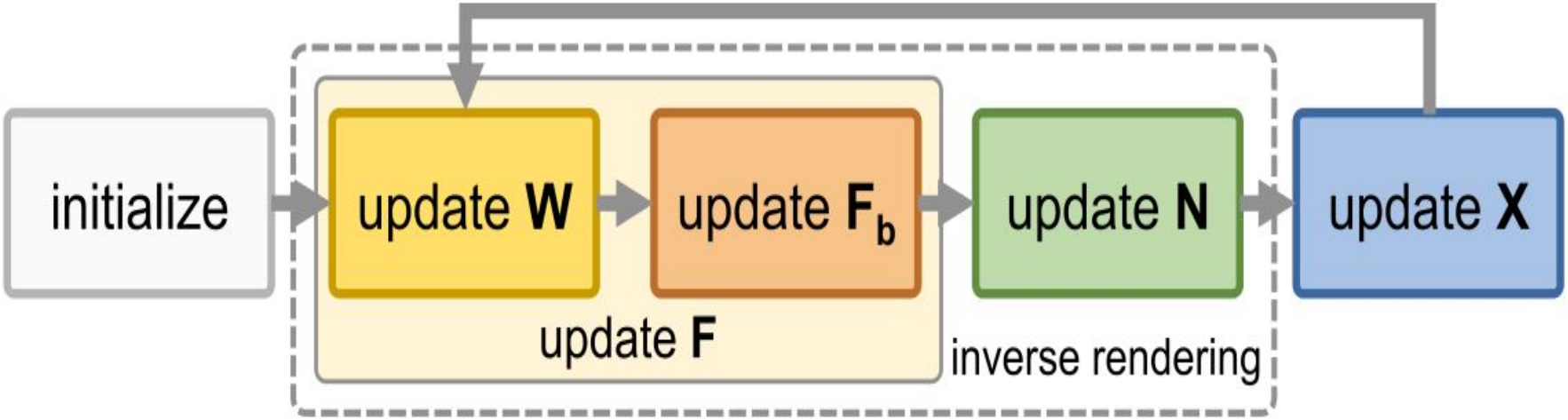

Figure 11. Overview of the algorithm, Adapted from *Practical SVBRDF Acquisition of 3D Objects with Unstructured Flash Photography,* by Nam et al., 2018, retrieved from https://dl.acm.org/doi/10.1145/3272127.3275017

4. Method in Detail

- Image Formation Model
- Reconstructing the SVBRDF
- Reconstructing the Normals
- Geometry Update

$$[m_i,\ 1]^T = \pi\ [R|t][M_i,\ 1]^T$$

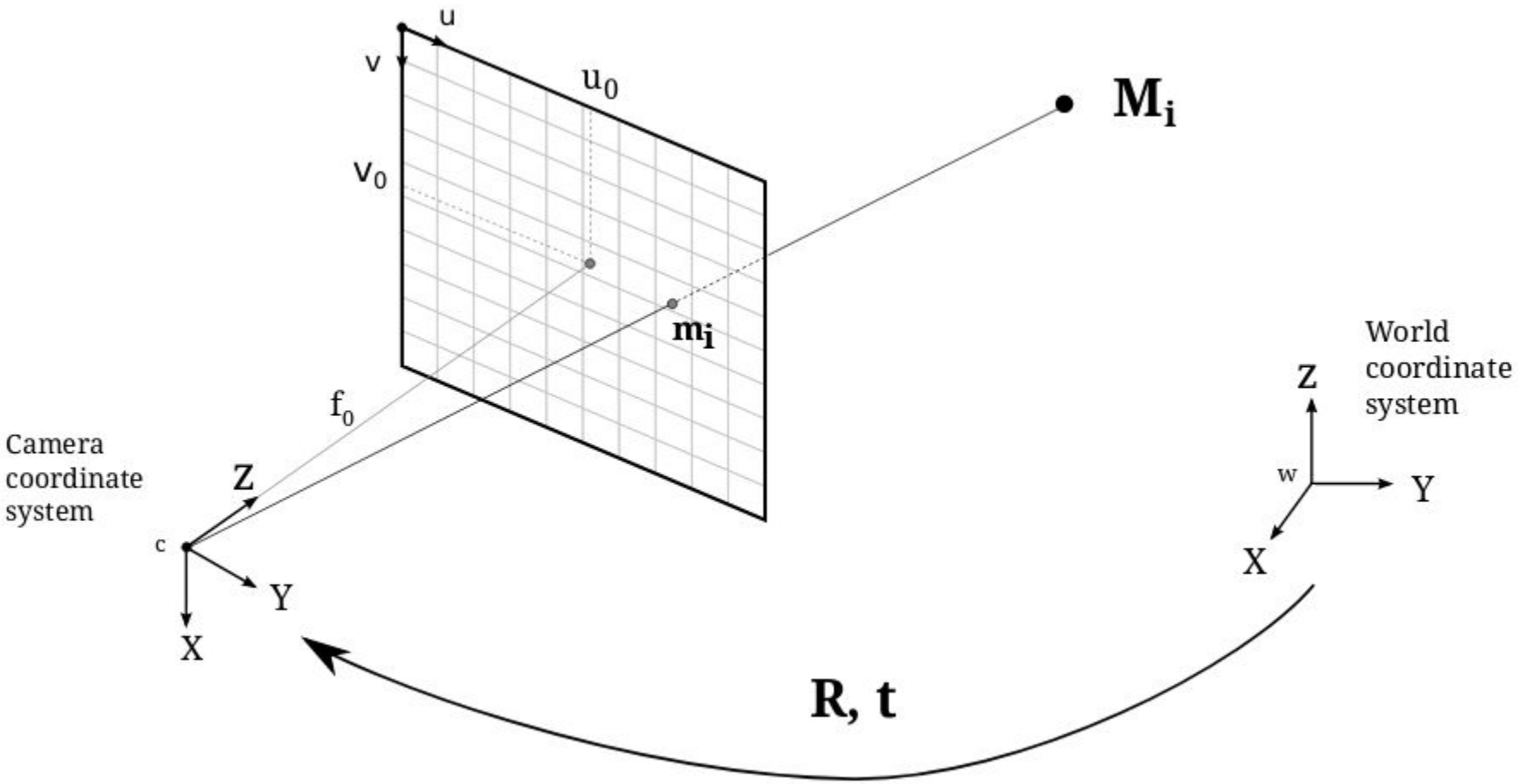

Figure 12. Pinhole Camera, Adapted from Kornia Documentation, 2019, retrieved from https://kornia.readthedocs.io/en/latest/_images/pinhole_model.png

Between 100 – 400 images are captured per object.

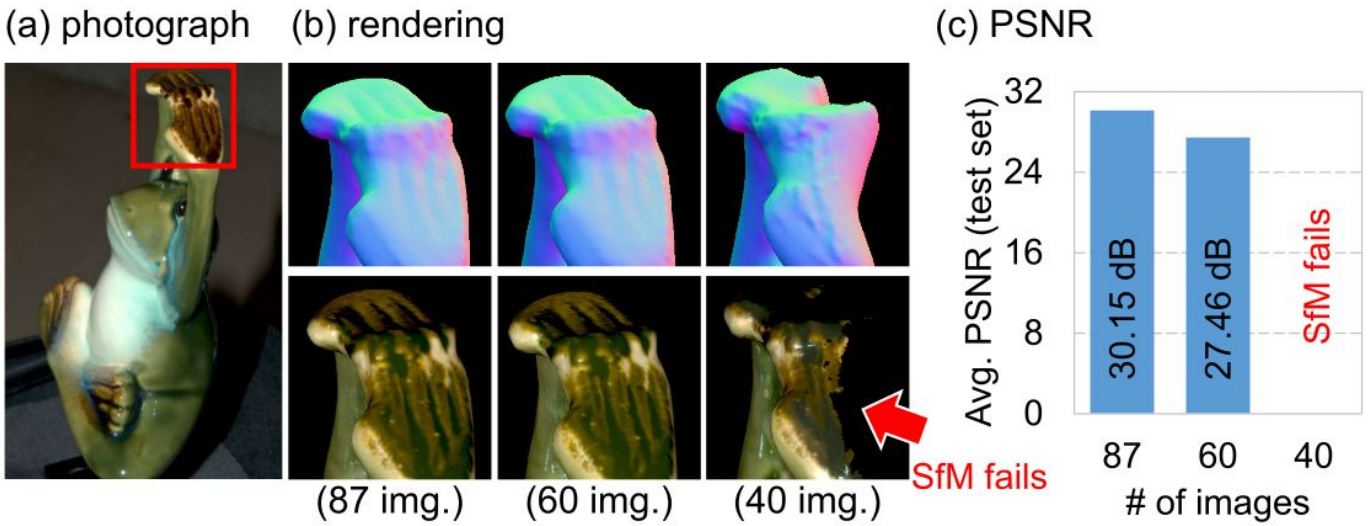

Figure 13. Impact of the number of input images, Adapted from *Practical SVBRDF Acquisition of 3D Objects with Unstructured Flash Photography,* by Nam et al., 2018, retrieved from https://dl.acm.org/doi/10.1145/3272127.3275017

What about recording a video instead of taking many pictures?

- motion blur
- inaccurate focus
- lower dynamic range of the still images

After having the camera parameters and the images, 3D dense point cloud is obtained by using MVS [Schönberger et al. 2016].

However MVS suffers from noise due to the reflection created by flash photography. Reflection violates diffuse reflectance assumption of MVS.

Therefore, initial geometry is modified further with screened Poisson surface reconstruction [Kazhdan and Hoppe 2013].

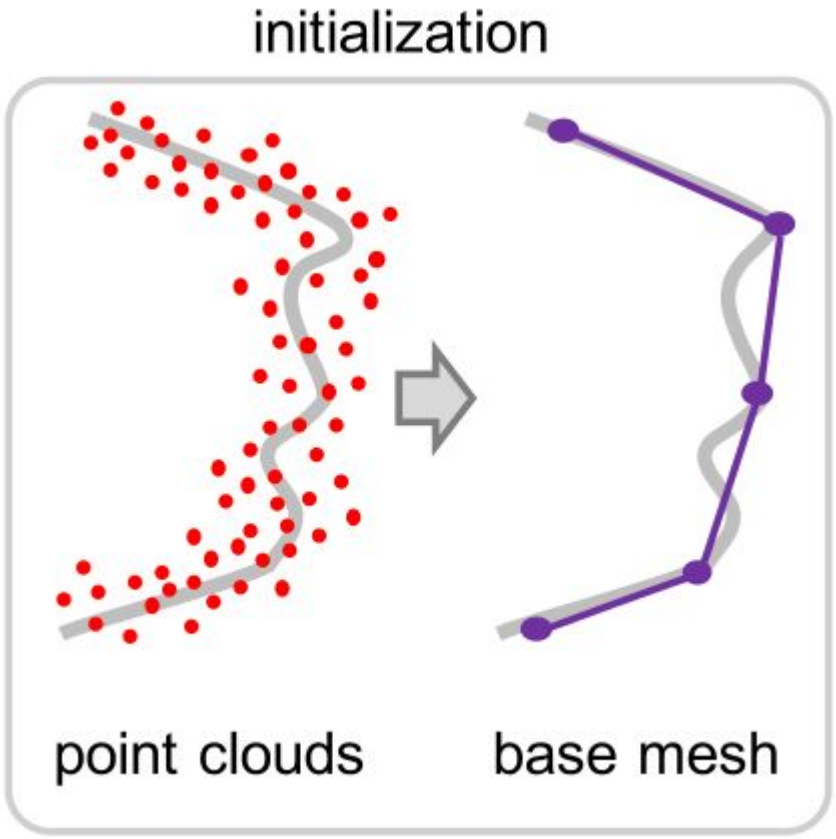

Figure 14. Initializing 3D geometry, Adapted from *Practical SVBRDF Acquisition of 3D Objects with Unstructured Flash Photography,* by Nam et al., 2018, retrieved from https://dl.acm.org/doi/10.1145/3272127.3275017

Image Formation Model

Image formation model proposed by Debevec and Malik [1997] is used,

$$I(\mathbf{u}) = L(\mathbf{o};\mathbf{x})\Delta t \Delta g$$

Reflectance function at point x is captured with the following formula,

$$L(\mathbf{o};\mathbf{x}) = f\,(\mathbf{i},\mathbf{o};\mathbf{x},\mathbf{n})\,L(-\mathbf{i};\mathbf{x})(\mathbf{n}\cdot\mathbf{i})$$

Reconstructing the SVBRDF

SVBRDF is represented by basis BRDFs and spatial weights.

$$\mathbf{F} = \left\{ f\left(\mathbf{i}, \mathbf{o}; \mathbf{x}_p\right) \right\} = \left\{ \sum_{b=1}^{B} \omega_{p,b} f_b\left(\mathbf{i}, \mathbf{o}\right) \right\}$$

Variables of the reflectance function are changed as in the work of Rusinkiewicz et.al. [1998] in order to obtain an efficient reparameterization.

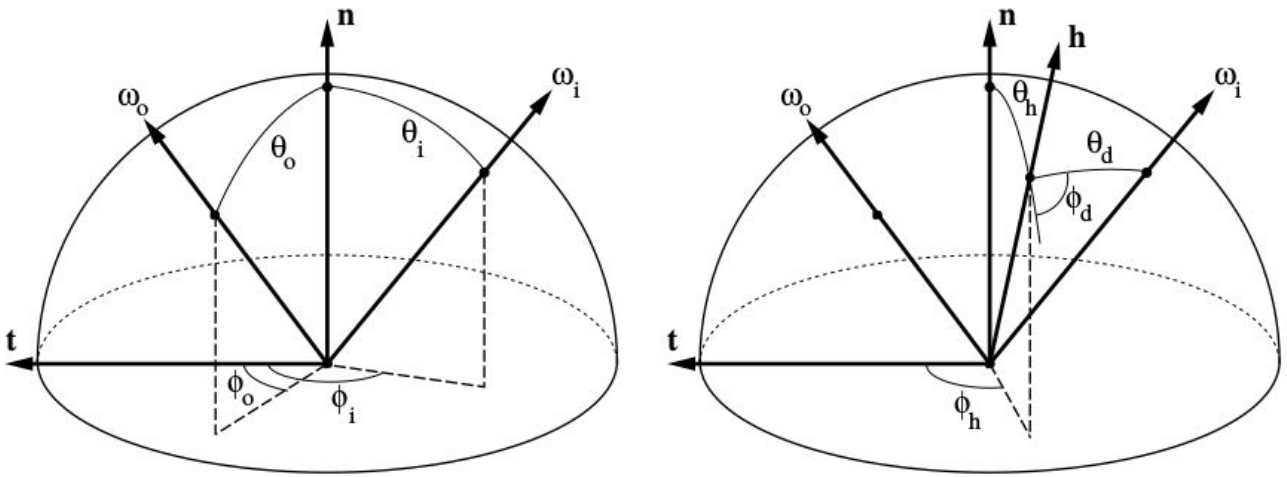

Figure 15. Proposed reparameterization of BRDFs, Adapted from *A New Change of Variables for Efficient BRDF Representation,* by Rusinkiewicz, 2011, retrieved from http://graphics.stanford.edu/papers/brdf_change_of_variables/brdf_change_of_variables.pdf

Dense sampling is obtained along the inclination angle of the halfway vector θ_h and the azimuthal angle φ_d of the difference vector but not along the inclination angle of the difference vector θ_d.

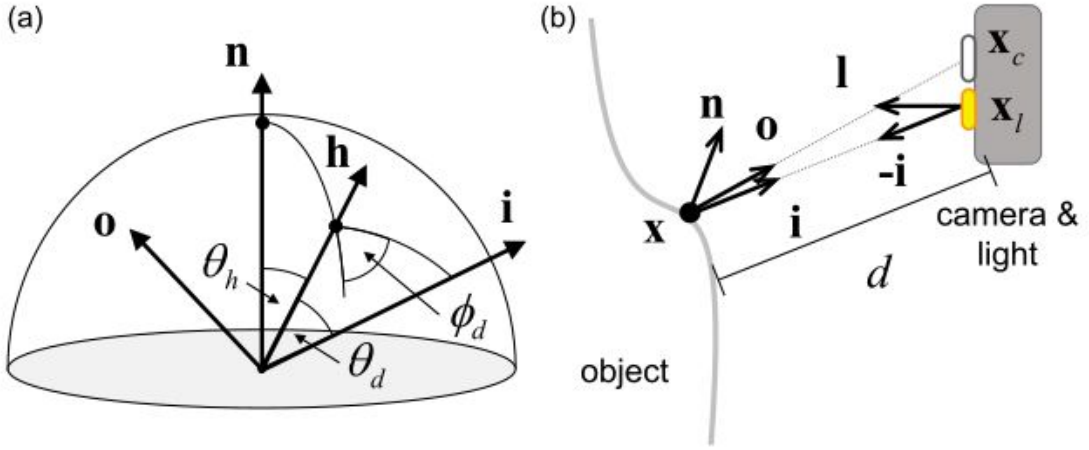

Figure 16. Rusinkiewicz parameterization and Geometry of the setup with a smartphone, Adapted from *Practical SVBRDF Acquisition of 3D Objects with Unstructured Flash Photography,* by Nam et al., 2018, retrieved from https://dl.acm.org/doi/10.1145/3272127.3275017

Slightly modified version of Cook-Torrance (CT) model [1982] is used to represent the basis BRDFs.

$$f_b(\mathbf{i},\mathbf{o}) = \frac{\rho_d}{\pi} + \rho_s \frac{D(\mathbf{h})G(\mathbf{n},\mathbf{i},\mathbf{o})F(\mathbf{h},\mathbf{i})}{4(\mathbf{n}\cdot\mathbf{i})(\mathbf{n}\cdot\mathbf{o})}$$

ρ_d and ρ_s are the diffuse and specular albedos.

D is a tabulated function $D(\theta_h) \in R^M$

G is the geometric term

F is the Fresnel term

Reflectance $f'_{p,k}$ is calculated with the formulas mentioned in image formation model and decomposed further as follows.

$$f'_{p,k} = \Phi^{\mathsf{T}}_{p,k} f_p$$

$$f_p = \sum_{b=1}^{B} \omega_{p,b} f_b$$

Basis BRDFs from the previous slide are represented as coefficient vectors

$$f_b = [\rho_d , \rho_s . F . D(\theta_h)] \in R^{M+1}$$

$\Phi_{p,k} \in R^{M+1}$ is the measurement vector specifying the sampled θ_h angles and the geometric factor $G/(4(n \cdot i)(n \cdot o))$ per pixel observation

A minimization problem is defined over all images (K) and all vertex points (P) by putting all together.

$$\underset{\mathbf{F}_b, \mathbf{W}}{\text{minimize}} \sum_{p=1}^{P} \sum_{k=1}^{K} v_{p,k} \left(f'_{p,k} - \mathbf{\Phi}^{\mathsf{T}}_{p,k} \sum_{b=1}^{B} \omega_{p,b} \boldsymbol{f}_b \right)^2$$

In order to update F_b , this problem is minimized with fixed W.

In order to find the optimal W, rough initial weights are calculated by using K-Means clustering w.r.t. the initial F_b values found by observing median brightness per vertex.

Cluster number K is found empirically.

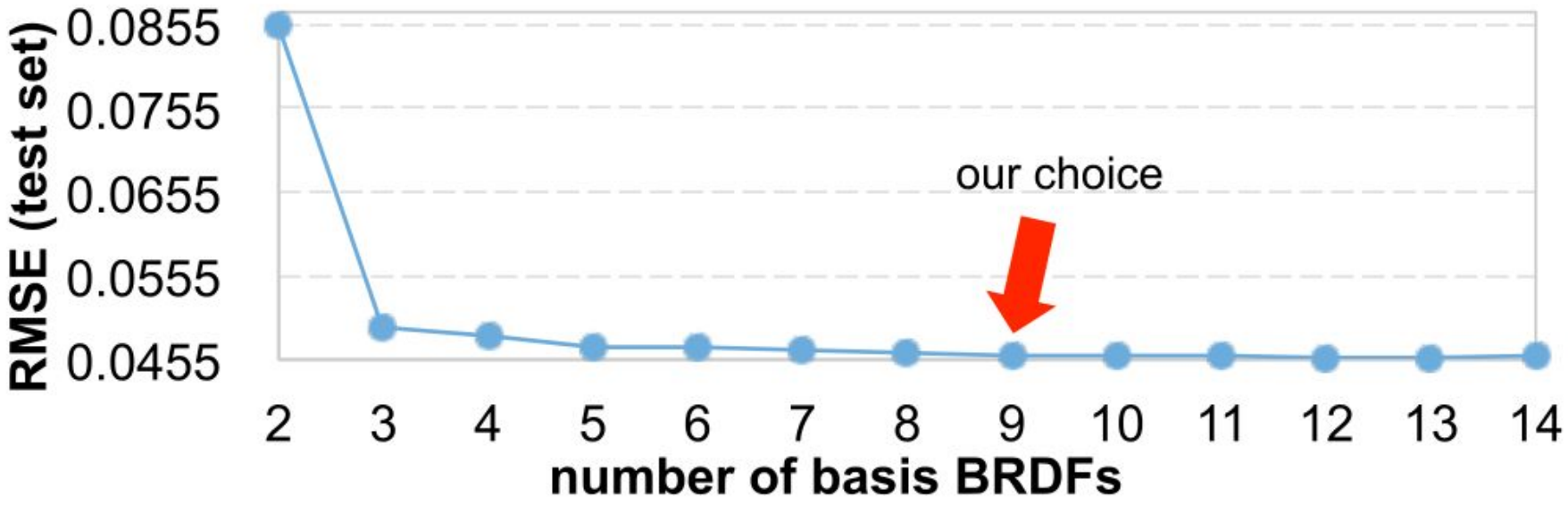

Figure 17. Impact of the number of basis BRDFs., Adapted from *Practical SVBRDF Acquisition of 3D Objects with Unstructured Flash Photography,* by Nam et al., 2018, retrieved from https://dl.acm.org/doi/10.1145/3272127.3275017

In order to update W , this time same problem is minimized with fixed F_b.

$$\underset{\mathbf{F}_b, \mathbf{W}}{\text{minimize}} \sum_{p=1}^{P} \sum_{k=1}^{K} v_{p,k} \left(f'_{p,k} - \mathbf{\Phi}^{\mathsf{T}}_{p,k} \sum_{b=1}^{B} \omega_{p,b} \boldsymbol{f}_b \right)^2$$

Reconstructing the Normals

$$O = \sum_{p=1}^{P} \sum_{k=1}^{K} v_{p,k} \left(L(\mathbf{o}_{p,k}; \mathbf{x}_p) - f(\mathbf{i}_{p,k}, \mathbf{o}_{p,k}; \mathbf{x}_p, \mathbf{n}_p) L(-\mathbf{i}_{p,k}; \mathbf{x}_p) (\mathbf{n}_p \cdot \mathbf{i}_{p,k}) \right)^2$$

After basis BRDFs and weights are estimated, reverse-rendering problem is optimized w.r.t. n_p.

Current surface normals $\{n_p\}$ are used for initialization. As long as radiances, directions and reflections of vertices are all known shading normals $\{\tilde{n}_p\}$ can be found by a standard linear least squares regression.

Geometry Update

After obtaining SVBRDF and shading normals, 3D geometry need to be updated in order to agree with the gained knowledge.

Screened Poisson surface reconstruction and marching cubes [Kazhdan and Hoppe 2013] methods are used to update the geometry.

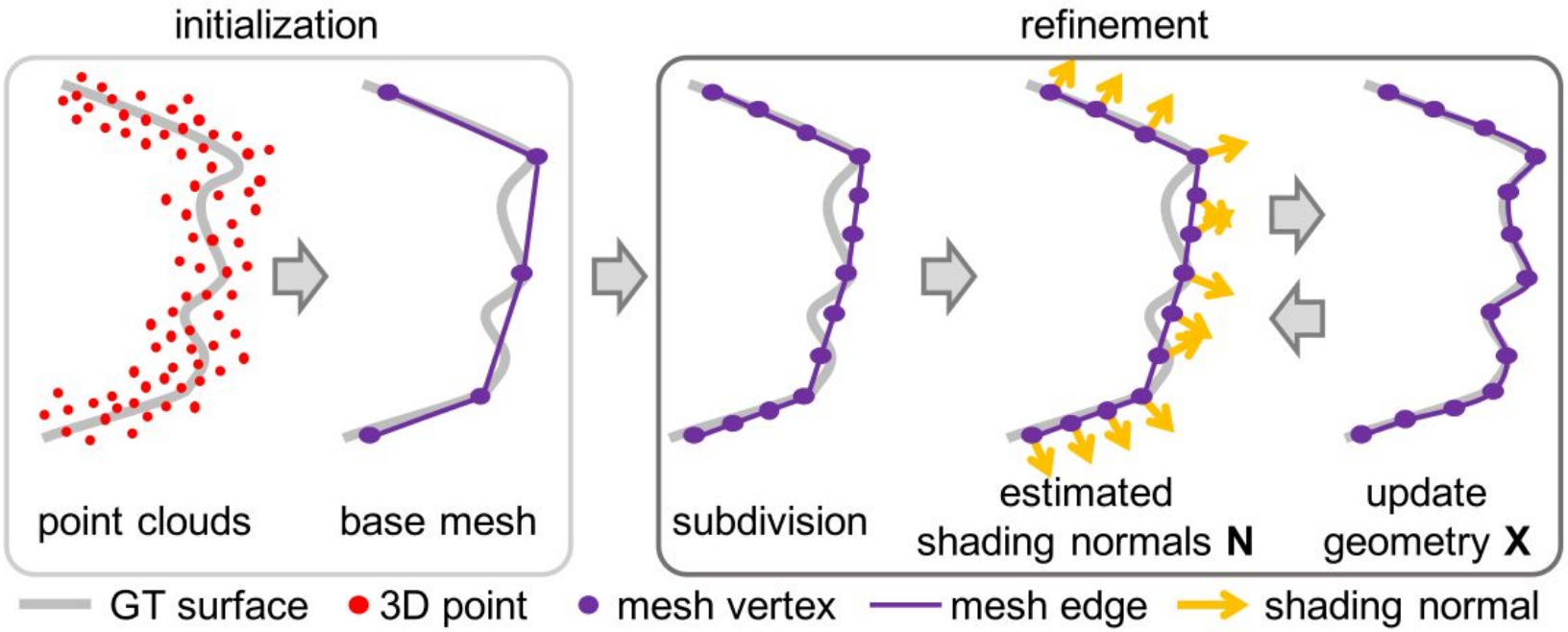

Figure 18. Updating 3D geometry, Adapted from *Practical SVBRDF Acquisition of 3D Objects with Unstructured Flash Photography*, by Nam et al., 2018, retrieved from https://dl.acm.org/doi/10.1145/3272127.3275017

SVBRDF, shading normals and geometry are updated until convergence.

In order to evaluate the geometry Hausdorff distance [Cignoni et al. 1998] between the previous mesh and the new X is used.

$$d_{\mathrm{H}}(X,Y) = \max\left\{ \sup_{x\in X}\inf_{y\in Y} d(x,y),\ \sup_{y\in Y}\inf_{x\in X} d(x,y) \right\}$$

Captured images are separated into training and testing groups and test RMS error of the photometric difference is used to decide whether to continue or stop.

5. Results and Evaluation

Figure 19. Results of the acquisition, Adapted from *Practical SVBRDF Acquisition of 3D Objects with Unstructured Flash Photography*, by Nam et al., 2018, retrieved from https://dl.acm.org/doi/10.1145/3272127.3275017

Validation of the BRDF Model

MERL BRDF dataset is used to validate the calculated reflectance values.

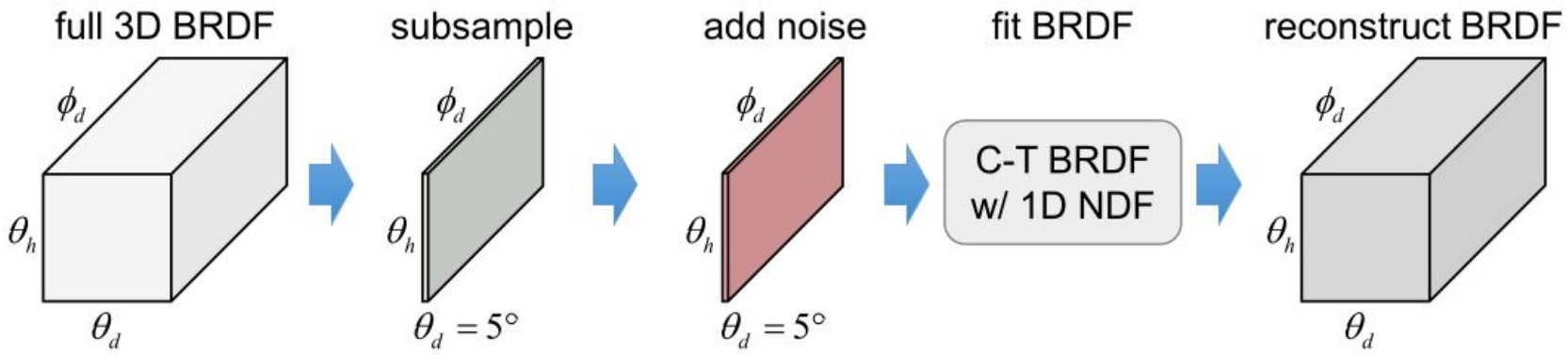

Figure 20. Validation experiment design for BRDF reconstruction method, Adapted from *Practical SVBRDF Acquisition of 3D Objects with Unstructured Flash Photography*, by Nam et al., 2018, retrieved from https://dl.acm.org/doi/10.1145/3272127.3275017

Validation of the Geometry

Geometry is compared against a setup with commercial 3D desktop scanner NextEngine and the state of the art 3D reconstruction method COLMAP [Schönberger 2016].

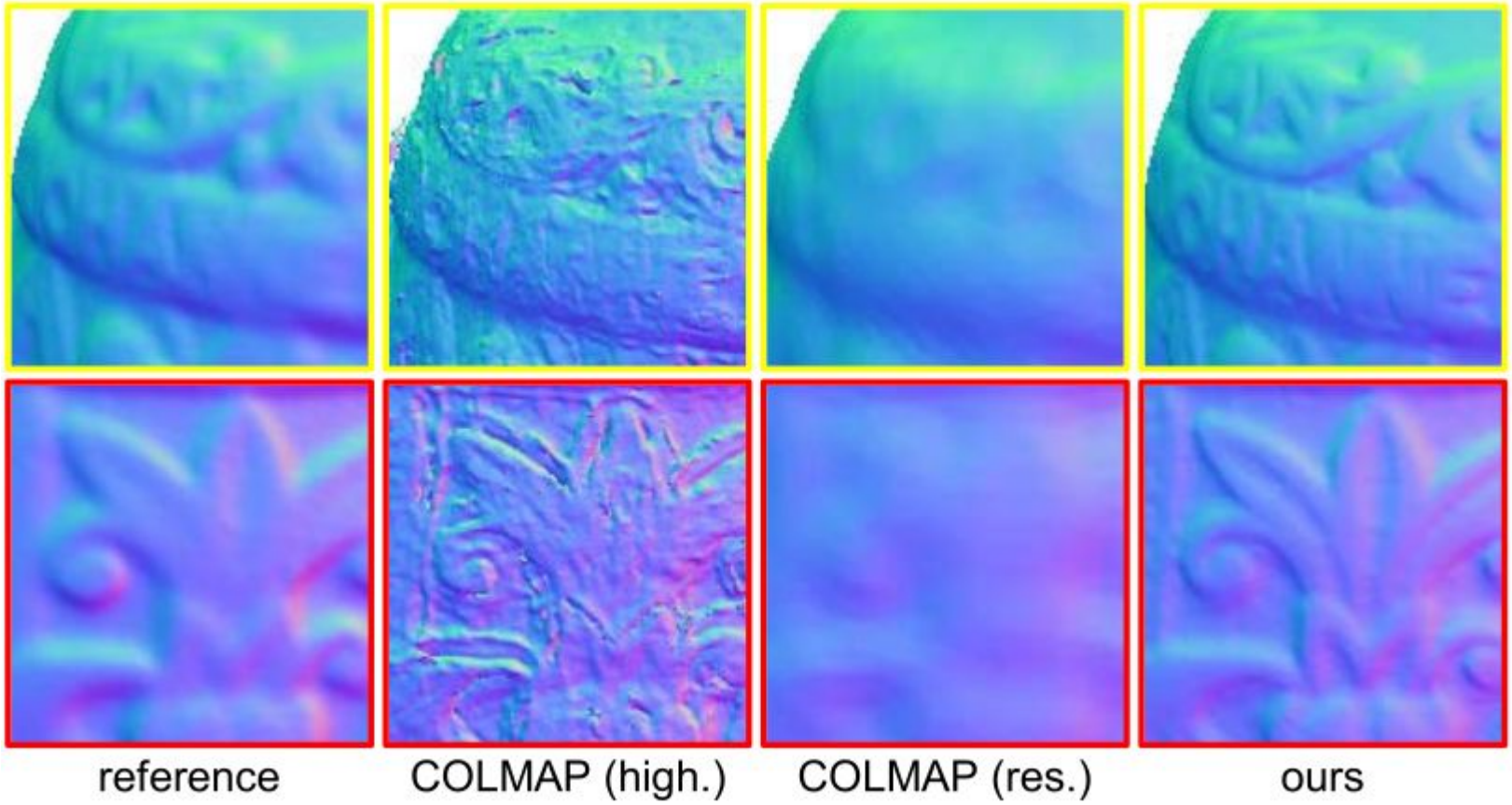

Figure 21. Comparison of geometric reconstruction with a reference geometry, *Adapted from Practical SVBRDF Acquisition of 3D Objects with Unstructured Flash Photography,* by Nam et al., 2018, retrieved from https://dl.acm.org/doi/10.1145/3272127.3275017

Proposed method yields a final reconstruction on-par with the professional 3D scanner if it uses low resolution result of the 3D scanning as initial geometry.

Figure 22. Comparison of geometric reconstruction with a reference geometry, Adapted from *Practical SVBRDF Acquisition of 3D Objects with Unstructured Flash Photography*, by Nam et al., 2018, retrieved from https://dl.acm.org/doi/10.1145/3272127.3275017

Performance

Desktop PC with the specified hardware as follows,

CPU	Intel i7-3770 3.40 GHz
Memory	32 GB
GPU	NVIDIA GTX1080

Each step of the initialization for obtaining the base rough geometry and extrinsic camera parameters approximately takes:

SFM	5 minutes
MVS	2 – 4 hours
Meshing	1 minute
One iteration	10 minutes

6. Limitations

- All surface points may not be captured properly.
- Image-based 3D modeling techniques may not capture complex geometries like pinecones accurately.
- SVBRDF does not take into account interreflections, subsurface scattering, nor transparency in our light transport model.

7. Conclusion

To sum up, authors offer a practical solution to obtain state-of-the-art acquisition of spatially varying reflectance and 3D geometry simultaneously by just using off -the-shelf cameras while similar works usually require more complex hardware.

Figure 23. Results of the acquisition, Adapted from *Practical SVBRDF Acquisition of 3D Objects with Unstructured Flash Photography*, by Nam et al., 2018, retrieved from https://dl.acm.org/doi/10.1145/3272127.3275017

References

Michael Kazhdan and Hugues Hoppe. 2013. Screened poisson surface reconstruction. ACM Transactions on Graphics (TOG) 32, 3 (2013), 29.

Jérémy Riviere, Pieter Peers, and Abhijeet Ghosh. 2015. Mobile Surface Reflectometry. Computer Graphics Forum (2015).

Zhuo Hui, Kalyan Sunkavalli, Joon-Young Lee, Sunil Hadap, Jian Wang, and Aswin Sankaranarayanan. 2017. Reflectance Capture Using Univariate Sampling of BRDFs. In Proc. IEEE Conference on Computer Vision and Pattern Recognition (CVPR). 5362–5370.

Tomoaki Higo, Yasuyuki Matsushita, Neel Joshi, and Katsushi Ikeuchi. 2009. A hand-held photometric stereo camera for 3-d modeling. In Computer Vision, 2009 IEEE 12th International Conference on. IEEE, 1234–1241.

Jaesik Park, Sudipta Sinha, Yasuyuki Matsushita, Yu Wing Tai, and In So Kweon. 2016. Robust Multiview Photometric Stereo using Planar Mesh Parameterization. IEEE Transactions on Pattern Analysis and Machine Intelligence (2016).

Johannes L. Schönberger. 2016. COLMAP. https://colmap.github.io.

Johannes L Schönberger, Enliang Zheng, Jan-Michael Frahm, and Marc Pollefeys. 2016. Pixelwise view selection for unstructured multi-view stereo. In European Conference on Computer Vision. Springer, 501–518.

Paul E. Debevec and Jitendra Malik. 1997. Recovering High Dynamic Range Radiance Maps from Photographs. In Proc. ACM SIGGRAPH ’97. 369–378.

Szymon Rusinkiewicz. 1998. A New Change of Variables for Efficient BRDF Representation. In Rendering Techniques ’98 (Proceedings of Eurographics Rendering Workshop ’98), G. Drettakis and N. Max (Eds.). Springer Wien, 11–22.

References

Robert L. Cook and Kenneth E. Torrance. 1982. A Reflectance Model for Computer Graphics. ACM Transactions on Graphics (TOG) 1, 1 (1982), 7–24. https://doi.org/10.1145/357290.357293

Paolo Cignoni, Claudio Rocchini, and Roberto Scopigno. 1998. Metro: Measuring error on simplified surfaces. In Computer Graphics Forum, Vol. 17. Wiley Online Library, 167–174.

Weyrich, Tim, et al. Principles of appearance acquisition and representation. Now Publishers Inc, 2009.

Weinmann, Michael, and Reinhard Klein. "Advances in geometry and reflectance acquisition (course notes)." SIGGRAPH Asia 2015 Courses. 2015. 1-71.

Nam, Giljoo, et al. "Practical SVBRDF acquisition of 3D objects with unstructured flash photography." ACM Transactions on Graphics (TOG) 37.6 (2018): 1-12.